Quadrature Measurement Characterization for Single-Mode Photon-Varied Gaussian States

Federico Forzano*, Andrea Giani*, Stefano Marano†, Moe Z. Win‡, and Andrea Conti*

*Department of Engineering and CNIT, University of Ferrara, Italy
†Department of Information and Electrical Engineering, University of Salerno, Italy
‡Laboratory for Information and Decision Systems, Massachusetts Institute of Technology, USA
E-mails: federico.forzano@unife.it, andrea.giani@unife.it, marano@unisa.it, moewin@mit.edu, a.conti@ieee.org

***Abstract*—Quantum systems for sensing, communication, control, and computing are pivotal for applications involving quantum networks. Such systems can perform quadrature measurements to extract information of interest inherent in the quantum states. Therefore, the design of quantum states is crucial to achieving high accuracy of the quadrature measurement. The widely used Gaussian states lack some relevant non-classical properties, thus calling for the design of quantum systems using non-Gaussian states. This paper characterizes the quadrature measurement accuracy for the photon-varied Gaussian states (PVGSs), which are a class of non-Gaussian states that can be generated using current technologies and possess relevant non-classical properties. First, we derive the wavefunctions of single-mode PVGSs. Then, we characterize the quadrature measurement accuracy and compare it with that for Gaussian states. The findings of this paper provide insights into the design of enhanced quantum systems and networks using single-mode PVGSs.**

***Index Terms*—Quantum information systems, quadrature measurements, electromagnetic radiation, non-Gaussian quantum states, photon-varied Gaussian states.**

I. Introduction

Quantum systems that use quantized electromagnetic radiations to perform quantum sensing [1]–[3], quantum communication [4]–[7], quantum control [8]–[10], and quantum computing [11]–[13] underpin various applications involving quantum networks. To accomplish their demanded tasks, these systems leverage on quantum mechanical phenomena, such as entanglement and superposition, and properly manipulate the physical properties of the employed quantum states [14]–[19]. In such applications, quadrature measurement of the quantum states can be performed to extract the information inherent in their associated electromagnetic radiations. However, this is a challenging task due to two main reasons. First, it requires the identification and the design of quantum states with suitable physical properties, while ensuring adequate measurement accuracy to meet applications requirements. Second, measuring the quadrature operators may be difficult due to the fragile nature of quantum states.

Quantum systems employing Gaussian states have been receiving particular interest owing to their solid and simple theoretical foundations and to the adequate maturity of technologies necessary to generate them [20]–[22]. The extensive use of Gaussian states is also attributed to the possibility of measuring their quadratures via optical homodyne or heterodyne detection [23], [24]. For example, [25] shows that a low-variance quadrature measurement is essential to ensuring adequate fault tolerance of a network-on-chip that connects the modules of a quantum computer. However, Gaussian states possess limited non-classical properties (e.g., they do not exhibit a negative Wigner function), which are essential to unleashing the full potential of quantum systems [26]–[28]. In this regard, non-Gaussian states can mitigate such a limitation, thus making them appealing for future quantum networks. Within the domain of non-Gaussian states, photon-varied Gaussian states (PVGSs) (a subclass of the photon-varied quantum states [29]) are receiving particular interest because they can be realized using current technologies with increasing efficiency [30]–[33]. In the literature, subclasses of PVGSs have been shown to provide significant performance gains over Gaussian states in quantum state discrimination [34], quantum sensing [5], [35], and quantum communication [36]–[40]. However, a general and detailed characterization of the accuracy with which the quadratures of PVGSs can be measured is still missing. In this regard, this paper addresses the following fundamental question: may PVGSs be used to enhance the accuracy when performing quadrature measurement? The answer to this question provides insights into the design of enhanced quantum networks. The key contributions of this paper can be summarized as follows:

- derivation of closed-form expressions for the wavefunctions of single-mode PVGSs; and
- characterization and quantification of the quadrature measurement accuracy for several subclasses of PVGSs.

The remaining sections are organized as follows. Section II recalls PVGSs and their Fock representation. Section III derives closed-form expressions for the wavefunctions of PVGSs, characterizes the variance of their quadrature measurement, and discusses interesting operating regimes. Finally, Section IV gives our conclusions.

Notation: Operators are denoted by bold uppercase letters. Sets are denoted by upright sans serif font except for the sets of natural numbers, integer numbers, real numbers, and complex numbers, which are denoted by $\mathbb{N}$, $\mathbb{Z}$, $\mathbb{R}$, and $\mathbb{C}$, respectively. For $n \in \mathbb{Z}$, $\overline{n}\!| = +$ for $n \geqslant 0$, and $\overline{n}\!| = -$

for $n < 0$. For $x \in \mathbb{R}$, $\lfloor x \rfloor$ denotes the greatest integer less than or equal to x. For $z \in \mathbb{C}$, $|z|$ denotes its absolute value, $\angle z$ denotes its angle, z^* denotes its complex conjugate, and $\imath = \sqrt{-1}$. For $z \in \mathbb{C}$, the principal branch of the complex square root is chosen such that $\sqrt{z} \triangleq |z|^{1/2} \exp\{\imath (\angle z)/2\}$. For a matrix $\boldsymbol{M}$, $[\boldsymbol{M}]_{i,j}$ denotes the element in the i-th row and j-th column. The adjoint of an operator is denoted by $(\cdot)^\dagger$. The annihilation and creation operators are denoted by $\boldsymbol{A}$ and $\boldsymbol{A}^\dagger$, respectively. The quadrature operators, namely the position and momentum operators, are $\boldsymbol{Q} \triangleq (\boldsymbol{A}^\dagger + \boldsymbol{A})/\sqrt{2}$ and $\boldsymbol{P} \triangleq \imath(\boldsymbol{A}^\dagger - \boldsymbol{A})/\sqrt{2}$, respectively. The set of density operators defined on a Hilbert space $\mathcal{H}$ is denoted by $\mathcal{D}(\mathcal{H})$. The identity operator defined on $\mathcal{H}$ is denoted by $\boldsymbol{I}_{\mathcal{H}}$. For two operators $\boldsymbol{X}$ and $\boldsymbol{Y}$, the commutator is denoted by $[\![\boldsymbol{X}, \boldsymbol{Y}]\!]_- \triangleq \boldsymbol{X}\boldsymbol{Y} - \boldsymbol{Y}\boldsymbol{X}$. The rotation operator with parameter $\phi \in \mathbb{R}$ is $\boldsymbol{R}_\phi \triangleq \exp\{\imath\phi\boldsymbol{A}^\dagger\boldsymbol{A}\}$. The displacement operator with parameter $\mu \in \mathbb{C}$ is $\boldsymbol{D}_\mu \triangleq \exp\{\mu\boldsymbol{A}^\dagger - \mu^*\boldsymbol{A}\}$. The squeezing operator with parameter $\zeta \in \mathbb{C}$ is $\boldsymbol{S}_\zeta \triangleq \exp\{\frac{1}{2}\zeta(\boldsymbol{A}^\dagger)^2 - \frac{1}{2}\zeta^*\boldsymbol{A}^2\}$.

II. Photon-Varied Gaussian States

This section presents some preliminaries on PVGSs that will be used to characterize their quadrature measurement.

A. Definition

Consider a single-mode of the quantized electromagnetic field, with underlying Hilbert space $\mathcal{H}$ and endowed with the creation and annihilation operators $\boldsymbol{A}^\dagger$ and $\boldsymbol{A}$ satisfying the canonical commutation relation $[\![\boldsymbol{A}, \boldsymbol{A}^\dagger]\!]_- = \boldsymbol{I}_{\mathcal{H}}$. The Hilbert space $\mathcal{H}$ is spanned by the Fock basis $\{|n\rangle\}_{n\in\mathbb{N}}$, where $|n\rangle$ is the Fock state with n photons. Consider a mixed Gaussian state $\boldsymbol{\Xi}(\phi, \mu, \zeta, \bar{n}) \in \mathcal{D}(\mathcal{H})$ defined as

$$\boldsymbol{\Xi}(\phi, \mu, \zeta, \bar{n}) \triangleq \boldsymbol{R}_\phi \boldsymbol{D}_\mu \boldsymbol{S}_\zeta \boldsymbol{\Xi}_{\text{th}}(\bar{n}) \boldsymbol{S}_\zeta^\dagger \boldsymbol{D}_\mu^\dagger \boldsymbol{R}_\phi^\dagger \tag{1}$$

where $\boldsymbol{\Xi}_{\text{th}}(\bar{n}) \in \mathcal{D}(\mathcal{H})$ is the thermal state

$$\boldsymbol{\Xi}_{\text{th}}(\bar{n}) \triangleq \sum_{n=0}^{\infty} \frac{\bar{n}^n}{(1+\bar{n})^{n+1}} |n\rangle\langle n| \tag{2}$$

with mean number of photons $\bar{n}$. In particular, $\bar{n}$ is given by the Planck's law $\bar{n} = (\exp\{\hbar\omega/(k_{\text{B}}T)\} - 1)^{-1}$, where $\hbar$ is the reduced Planck constant, ω is the angular frequency of the field, k_{B} is the Boltzmann constant, and T is the absolute temperature. Define the photon-variation operator $\boldsymbol{V}_{t]}$ as

$$\boldsymbol{V}_{t]} \triangleq \begin{cases} \boldsymbol{A} & \text{for } t = -1 \\ \boldsymbol{A}^\dagger & \text{for } t = +1 \end{cases} \tag{3}$$

where $t \in \{-1, +1\}$ distinguishes between photon-subtraction ($t = -1$) and photon-addition ($t = +1$). PVGSs constitute a general class of quantum states obtained applying k photon variation via $\boldsymbol{V}_{t]}^k$ to a Gaussian state $\boldsymbol{\Xi}(\phi, \mu, \zeta, \bar{n})$. A PVGS $\boldsymbol{\Xi}_{t]}^{(k)}(\phi, \mu, \zeta, \bar{n}) \in \mathcal{D}(\mathcal{H})$ with k photon-variation is defined as

$$\boldsymbol{\Xi}_{t]}^{(k)}(\phi, \mu, \zeta, \bar{n}) \triangleq \frac{\boldsymbol{V}_{t]}^k \boldsymbol{\Xi}(\phi, \mu, \zeta, \bar{n}) (\boldsymbol{V}_{t]}^\dagger)^k}{N_{t]}^{(k)}(\bar{n})} \tag{4}$$

where $N_{t]}^{(k)}(\bar{n})$ is the associated normalization constant ensuring that $\text{tr}\{\boldsymbol{\Xi}_{t]}^{(k)}(\phi, \mu, \zeta, \bar{n})\} = 1$ and given by [5, Eq. (32)]. PVGSs reduce to Gaussian states when $k = 0$; to photon-added Gaussian states (PAGSs) when $t = +1$ and $k > 0$; and to photon-subtracted Gaussian states (PSGSs) when $t = -1$, $k > 0$, and $\zeta \neq 0$. Furthermore, when $\bar{n} = 0$, $\boldsymbol{\Xi}_{\text{th}}(\bar{n}) = |0\rangle\langle 0|$ and $\boldsymbol{\Xi}_{t]}^{(k)}(\phi, \mu, \zeta, \bar{n})$ reduces to a pure PVGS $|\psi_{t]}^{(k)}(\phi, \mu, \zeta)\rangle \in \mathcal{H}$ defined as

$$\begin{aligned} |\psi_{t]}^{(k)}(\phi, \mu, \zeta)\rangle &\triangleq \frac{1}{N_{t]}^{(k)}} \boldsymbol{V}_{t]}^k \boldsymbol{R}_\phi \boldsymbol{D}_\mu \boldsymbol{S}_\zeta |0\rangle \\ &= \frac{1}{N_{t]}^{(k)}} \boldsymbol{V}_{t]}^k |\phi, \mu, \zeta\rangle \end{aligned} \tag{5}$$

where $|\phi, \mu, \zeta\rangle \in \mathcal{H}$ is a pure Gaussian state. The normalization constant $N_{t]}^{(k)}$ in (5) is related to $N_{t]}^{(k)}(\bar{n})$ in (4) via

$$N_{t]}^{(k)} = \lim_{\bar{n}\to 0} \sqrt{N_{t]}^{(k)}(\bar{n})}\,. \tag{6}$$

B. Fock representation of PVGSs

The Fock (number) representation of a single-mode PVGS $\boldsymbol{\Xi}_{t]}^{(k)}(\phi, \mu, \zeta, \bar{n})$ is

$$\boldsymbol{\Xi}_{t]}^{(k)}(\phi, \mu, \zeta, \bar{n}) = \sum_{n,m=0}^{\infty} c_{n,m} |n\rangle\langle m| \tag{7}$$

where $c_{n,m} = \langle n|\boldsymbol{\Xi}_{t]}^{(k)}(\phi, \mu, \zeta, \bar{n})|m\rangle$ are the Fock coefficients given by [5, Eq. (31)]. For the pure PVGS $|\psi_{t]}^{(k)}(\phi, \mu, \zeta)\rangle$, the Fock representation is given by (8) at the top of the next page, where $H_n(x)$ is the Hermite polynomial of degree n, while $\Lambda_{\mu,\zeta}$ and $\eta_{\mu,\zeta}$ are given respectively by

$$\begin{aligned} \Lambda_{\mu,\zeta} = &\sqrt{\text{sech}(|\zeta|)} \\ &\times \exp\left\{-\frac{1}{2}\Big(|\mu|^2 + (\mu^*)^2 \tanh(|\zeta|) e^{\imath(\angle\zeta + \pi)}\Big)\right\} \end{aligned} \tag{9}$$

$$\eta_{\mu,\zeta} = \frac{\mu + \mu^* \tanh(|\zeta|) e^{\imath(\angle\zeta+\pi)}}{\sqrt{2\tanh(|\zeta|) e^{\imath(\angle\zeta+\pi)}}}\,. \tag{10}$$

C. Experimental preparation

The relatively simple preparation of PVGSs is one of the main features that make them appealing for practical applications compared to other non-Gaussian states. The generation of PVGSs is of forwent interest in experimental optics, with experiments demonstrating photon-subtraction and photon-addition of up to four photons using versatile methods. For instance, [41] achieved four photon-subtraction at telecommunication wavelength squeezed light via transition-edge sensors. Similarly, [42] subtracted up to ten photons from thermal states using a single avalanche photodiode in a continuous-wave regime, leveraging long coherence times and low-reflectivity beam splitters to enable multiphoton conditioning. Recent advances also explore the generation of PAGSs: [30] produced multiphoton-added coherent states using conditional measurements, achieving high-fidelity preparation via probabilistic amplification.

$$|\psi_{\bar{t}|}^{(k)}(\phi,\mu,\zeta)\rangle = \frac{\Lambda_{\mu,\zeta}}{N_{\bar{t}|}^{(k)}} \sum_{n=0}^{\infty} \sqrt{\frac{(n+k)!}{n!\,(n-k\frac{t-1}{2})!}} \left(\frac{\tanh(|\zeta|)\, e^{\imath(\angle\zeta+2\phi+\pi)}}{2}\right)^{\frac{1}{2}(n-k\frac{t-1}{2})} H_{n-k\frac{t-1}{2}}(\eta_{\mu,\zeta})\,|n+k\frac{t+1}{2}\rangle \tag{8}$$

$$\psi_{\bar{t}|}^{(k)}(q|\phi,\mu,\zeta) = \frac{\Lambda_{\mu,\zeta}}{N_{\bar{t}|}^{(k)}} \frac{e^{\frac{\eta_{\mu,\zeta}^2\,\gamma_{\phi,\zeta}^2}{1+\gamma_{\phi,\zeta}^2}}\,\gamma_{\phi,\zeta}^{k\frac{1-t}{2}}}{\pi^{\frac{1}{4}}\,2^{\frac{k}{2}}\,(1-\gamma_{\phi,\zeta}^2)^{\frac{k+1}{2}}} \exp\left\{-\frac{\left(q-\frac{2\,\gamma_{\phi,\zeta}\,\eta_{\mu,\zeta}}{1+\gamma_{\phi,\zeta}^2}\right)^2}{2\,\frac{1-\gamma_{\phi,\zeta}^2}{1+\gamma_{\phi,\zeta}^2}}\right\} H_k\left((-1)^{\frac{1-t}{2}}\,\frac{\gamma_{\phi,\zeta}^{\frac{1-t}{2}}\,q-\gamma_{\phi,\zeta}^{\frac{1+t}{2}}\,\eta_{\mu,\zeta}}{\sqrt{1-\gamma_{\phi,\zeta}^2}}\right) \tag{12}$$

III. Quadrature Characterization of PVGSs

This section derives both the position and momentum wavefunctions of pure PVGSs and characterizes the variance when performing measurements on their quadratures. The wavefunctions are central to deriving the Wigner function [43].

A. Wavefunctions of pure PVGSs

The position wavefunction of a pure PVGS is defined as

$$\psi_{\bar{t}|}^{(k)}(q|\phi,\mu,\zeta) = \langle q|\psi_{\bar{t}|}^{(k)}(\phi,\mu,\zeta)\rangle \tag{11}$$

where $|q\rangle$ is an eigenstate of the position operator $\boldsymbol{Q}$, i.e., $\boldsymbol{Q}\,|q\rangle = q\,|q\rangle$. The following theorem derives the explicit expression for the position wavefunction in (11).

Theorem 1. The wavefunction $\psi_{\bar{t}|}^{(k)}(q|\phi,\mu,\zeta)$ of a pure PVGS $|\psi_{\bar{t}|}^{(k)}(\phi,\mu,\zeta)\rangle \in \mathcal{H}$ is given by (12) at the top of the page, where

$$\gamma_{\phi,\zeta} = \sqrt{\tanh(|\zeta|)e^{\imath(\angle\zeta+2\phi+\pi)}}\,. \tag{13}$$

□

Proof: Consider the wavefunction of a Fock state [43]

$$\psi_n(q) = \frac{1}{\sqrt{2^n\,n!}}\left(\frac{1}{\pi}\right)^{\frac{1}{4}} e^{-\frac{q^2}{2}} H_n(q)\,. \tag{14}$$

By using (8) and (14) in (11) and after some algebra, the left-hand side in (11) results in (15) at the top of the next page. Then, (12) follows by using [5, Eq. (5)] and by noticing that

$$n-k\frac{t-1}{2} = \begin{cases} n+k & \text{for } t=-1 \\ 0 & \text{for } t=+1 \end{cases} \tag{16}$$

$$n+k\frac{t+1}{2} = \begin{cases} 0 & \text{for } t=-1 \\ n+k & \text{for } t=+1\,. \end{cases} \tag{17}$$

⊠

For the same pure PVGS $|\psi_{\bar{t}|}^{(k)}(\phi,\mu,\zeta)\rangle$, the momentum wavefunction $\phi_{\bar{t}|}^{(k)}(p|\phi,\mu,\zeta)$ can be obtained from the Fourier transform of the position wavefunction $\psi_{\bar{t}|}^{(k)}(q|\phi,\mu,\zeta)$ as

$$\phi_{\bar{t}|}^{(k)}(p|\phi,\mu,\zeta) = \frac{1}{\sqrt{2\pi}}\int_{\mathbb{R}} \psi_{\bar{t}|}^{(k)}(q|\phi,\mu,\zeta)\,e^{-\imath pq}\,dq\,. \tag{18}$$

B. Variance of the Quadrature Measurement for PVGSs

Since the quadrature measurement is central in several applications, it is crucial to understand how the quadrature measurement variance behaves for a PVGS. In the following, we characterize the variance of the quadrature measurement for PVGSs as indicator of the accuracy. To accomplish this task, define

$$\boldsymbol{X}_a \triangleq \frac{\imath^a}{\sqrt{2}}(\boldsymbol{A}^\dagger + (-1)^a\boldsymbol{A}) \tag{19}$$

where $a \in \{0,1\}$. Specifically, $\boldsymbol{X}_0 = \boldsymbol{Q}$ and $\boldsymbol{X}_1 = \boldsymbol{P}$. The variance of $\boldsymbol{X}_a$ is

$$\langle(\Delta\boldsymbol{X}_a)^2\rangle = \langle\boldsymbol{X}_a^2\rangle - \langle\boldsymbol{X}_a\rangle^2. \tag{20}$$

For a mixed PVGS $\boldsymbol{\Xi}_{\bar{t}|}^{(k)}(\phi,\mu,\zeta,\bar{n})$, the computation of the variance of $\boldsymbol{X}_a$ requires deriving explicit expression for

$$\langle\boldsymbol{X}_a\rangle = \frac{\imath^a}{\sqrt{2}}\sum_{n=0}^{\infty}\sqrt{n+1}\,(c_{n,n+1}+(-1)^a\,c_{n+1,n}) \tag{21a}$$

$$\langle\boldsymbol{X}_a^2\rangle = (-1)^a\sum_{n=0}^{\infty}\sqrt{\frac{(n+2)!}{n!}}\,\mathrm{Re}\{c_{n,n+2}\} + \frac{N_{\bar{t}|}^{(k+1)}(\bar{n})}{N_{\bar{t}|}^{(k)}(\bar{n})} - \frac{t}{2}\,. \tag{21b}$$

When the state is pure, the explicit expressions for (21a) and (21b) are given in the following theorem.

Theorem 2. Let $|\psi_{\bar{t}|}^{(k)}(\phi,\mu,\zeta)\rangle \in \mathcal{H}$ be a pure PVGS. The explicit expression for $\langle\boldsymbol{X}_a\rangle$ and $\langle\boldsymbol{X}_a^2\rangle$ are given by (22a) and (22b) at the top of next page, in which the inner products between PVGSs are given by [5, Eqs. (42)-(45)]. □

Proof: By using (19) in (20), it follows that

$$\langle\boldsymbol{X}_a\rangle = \frac{\imath^a}{\sqrt{2}}(\langle\boldsymbol{A}^\dagger\rangle + (-1)^a\langle\boldsymbol{A}\rangle) \tag{23a}$$

$$\langle(\boldsymbol{X}_a)^2\rangle = \frac{(-1)^a}{2}\left[\langle(\boldsymbol{A}^\dagger)^2\rangle + \langle\boldsymbol{A}^2\rangle + (-1)^a\,(2\langle\boldsymbol{A}^\dagger\boldsymbol{A}\rangle+1)\right]. \tag{23b}$$

$$\psi_{\bar{t}|}^{(k)}(q|\phi,\mu,\zeta) = \frac{\Lambda_{\mu,\zeta}}{N_{\bar{t}|}^{(k)}} \sum_{n=0}^{\infty} \sqrt{\frac{(n+k)!}{n!(n-k\frac{t-1}{2})!}} \left(\frac{\tanh(|\zeta|)e^{\imath(\angle\zeta+2\phi+\pi)}}{2}\right)^{\frac{1}{2}(n-k\frac{t-1}{2})} H_{n-k\frac{t-1}{2}}(\eta_{\mu,\zeta}) \langle q|n+k\frac{t+1}{2}\rangle$$

$$= \frac{\Lambda_{\mu,\zeta}}{N_{\bar{t}|}^{(k)}} \left(\frac{1}{\pi}\right)^{\frac{1}{4}} e^{-\frac{q^2}{2}} \sum_{n=0}^{\infty} \sqrt{\frac{(n+k)!}{n!(n-k\frac{t-1}{2})!}} \left(\frac{\tanh(|\zeta|)e^{\imath(\angle\zeta+2\phi+\pi)}}{2}\right)^{\frac{1}{2}(n-k\frac{t-1}{2})}$$

$$\times \left(2^{n+k\frac{t-1}{2}}\,(n+k\frac{t+1}{2})!\right)^{-\frac{1}{2}} H_{n-k\frac{t-1}{2}}(\eta_{\mu,\zeta})\, H_{n+k\frac{t+1}{2}}(q) \tag{15}$$

$$\langle \boldsymbol{X}_a\rangle = \frac{\imath^{a(2-t)}}{\sqrt{2}} \frac{N_{\bar{t}|}^{(k+1)}}{N_{\bar{t}|}^{(k)}} \left(\langle\psi_{\bar{t}|}^{(k)}(\phi,\mu,\zeta)|\psi_{\bar{t}|}^{(k+1)}(\phi,\mu,\zeta)\rangle + (-1)^a \langle\psi_{\bar{t}|}^{(k+1)}(\phi,\mu,\zeta)|\psi_{\bar{t}|}^{(k)}(\phi,\mu,\zeta)\rangle\right) \tag{22a}$$

$$\langle(\boldsymbol{X}_a)^2\rangle = (-1)^a \frac{N_{\bar{t}|}^{(k+2)}}{N_{\bar{t}|}^{(k)}} \mathrm{Re}\Big\{\langle\psi_{\bar{t}|}^{(k)}(\phi,\mu,\zeta)|\psi_{\bar{t}|}^{(k+2)}(\phi,\mu,\zeta)\rangle\Big\} + \left(\frac{N_{\bar{t}|}^{(k+1)}}{N_{\bar{t}|}^{(k)}}\right)^2 - \frac{t}{2} \tag{22b}$$

Then, (22a) and (22b) are respectively obtained from (23a) and (23b), by using

$$\langle \boldsymbol{V}_{\bar{s}|}^{n}\rangle = \frac{N_{\bar{t}|}^{(k+n)}}{N_{\bar{t}|}^{(k)}} \langle\psi_{\bar{t}|}^{(k+n\frac{1-st}{2})}(\phi,\mu,\zeta)|\psi_{\bar{t}|}^{(k+n\frac{1+st}{2})}(\phi,\mu,\zeta)\rangle$$

$$\langle \boldsymbol{A}^\dagger \boldsymbol{A}\rangle = \left(\frac{N_{\bar{t}|}^{(k+1)}}{N_{\bar{t}|}^{(k)}}\right)^2 - \frac{1+t}{2}\,.$$

$\boxtimes$

Fig. 1 shows the variance $\langle(\Delta\boldsymbol{X}_0)^2\rangle$ of the position measurement for PVGSs as function of $|\mu|$. Solid lines represent PAGSs ($t=+1$), dashed lines represent PSGSs ($t=-1$), and different colors distinguish different numbers of photon-variations k. The squeezing parameter is set to $\zeta=-2/3$ in order to reduce the position variance and highlight the effect of photon-variations. For $k=0$, i.e., for a Gaussian state, the variance is constant and depends parametrically on the squeezing (e.g., for $|\zeta|=0$ the Gaussian state reduces to a coherent state with variance $1/2$). For $k>0$, i.e., when photon-variations are performed, the variance becomes dependent on the displacement amplitude $|\mu|$. Note that for fixed squeezing ζ, there exist values for μ and k such that the variance for PVGSs is lower than that of Gaussian states, yelding to a better accuracy of the quadrature measurement. However, such accuracy gain reduces for increasing $|\mu|$ and asymptotically vanishes when $|\mu|$ approaches infinity.

Fig. 2 shows the variance $\langle(\Delta\boldsymbol{X}_0)^2\rangle$ of the position measurement as a function of $|\zeta|$, where $\angle\zeta=\pi$ and $\mu=1$. For $k=0$, the variance monotonically decreases with $|\zeta|$. For $k>0$, Fig. 2 shows that PSGSs perform better than Gaussian states as long as $|\zeta|$ is sufficiently small. The plots also indicate that for each k, there exists an optimal squeezing that minimizes the variance. On the other hand, it can be observed that the variance achieved with PAGSs is always greater than that of Gaussian states, thus resulting in a worst measurement accuracy of the position operator. Analogously to Fig. 1, the variance of PVGSs approaches that of Gaussian states when $|\zeta|$ becomes sufficiently large.

Fig. 3 shows the variance $\langle(\Delta\boldsymbol{X}_1)^2\rangle$ of the momentum measurement for PVGSs as a function of $|\mu|$ for the same parameters used in Fig. 1. For $k=0$, the variance for the Gaussian state is constant and greater than $1/2$, as expected from the Heisenberg uncertainty principle. Furthermore, Fig. 3 shows that the momentum variance for PVGSs is higher than that of Gaussian states. This is still attributed to the Heisenberg principle, as the accuracy gain achieved for position measurements in Fig. 1 leads to a worst accuracy when measuring the momentum operator.

Finally, Fig. 4 shows the variance $\langle(\Delta\boldsymbol{X}_1)^2\rangle$ of the momentum measurement as a function of $|\zeta|$. As in Fig. 3, the plot shows that the variance for PVGSs increases with k and $|\zeta|$, being higher than that of Gaussian states as a consequence of the Heisenberg principle.

The numerical results show that using PVGSs is beneficial to the quadrature measurement accuracy. In particular, the plots show that for specific choices of k and t, there exist values for $|\mu|$ and $|\zeta|$ that allow PVGSs to provide a better quadrature measurement accuracy than Gaussian states.

IV. Conclusion

This paper characterized the accuracy of quadrature measurement for single-mode PVGSs by deriving closed-form expressions for the wavefunctions and the measurement variance. It introduced a new perspective on the use of PVGSs in quantum systems relying on quadrature measurement of quantized electromagnetic radiations. The findings of this work show that the additional degrees of freedom provided by PVGSs open to the possibility of designing optimized states for specific applications and operational regimes.

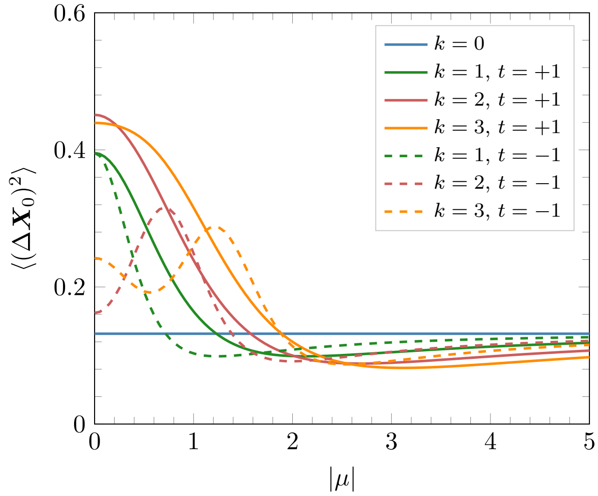

Fig. 1: Variance of the position measurement for PVGSs as a function of $|\mu|$, with a different number of photon-variations k. We set $\phi = 0$, $\angle\mu = 0$, and $\zeta = -2/3$.

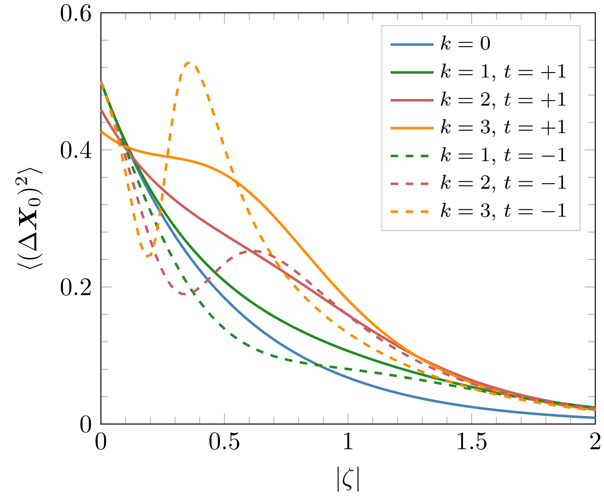

Fig. 2: Variance of the position measurement for PVGSs as a function of $|\zeta|$, with a different number of photon-variations k. We set $\phi = 0$, $\mu = 1$, and $\angle\zeta = \pi$.

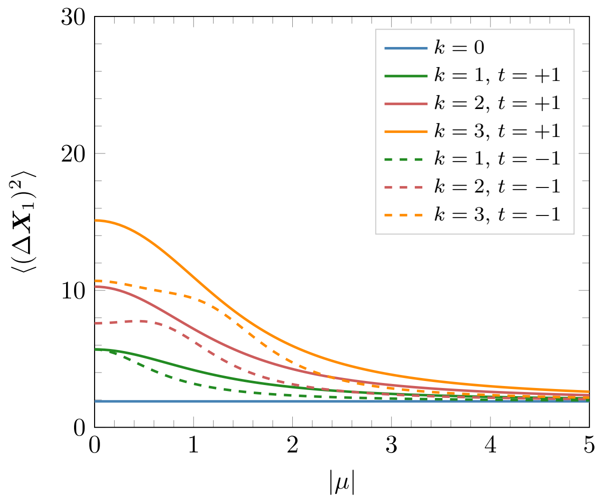

Fig. 3: Variance of the momentum measurement for PVGSs as a function of $|\mu|$, with a different number of photon-variations k. We set $\phi = 0$, $\angle\mu = 0$, and $\zeta = -2/3$.

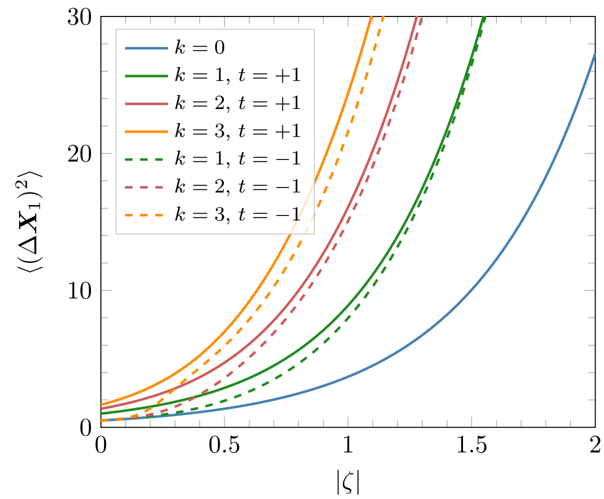

Fig. 4: Variance of momentum measurement for PVGSs as a function of $|\zeta|$, with a different number of photon-variations k. We set $\phi = 0$, $\mu = 1$, and $\angle\zeta = \pi$.

Acknowledgment

The fundamental research described in this paper was supported, in part, by the Ministero dell'Università e della Ricerca and NextGenerationEU under Grant No. 2022JES5S2, by the National Science Foundation under Grant No. CCF-1956211, and by the Robert R. Taylor Professorship.

References

[1] S. Lloyd, "Enhanced sensitivity of photodetection via quantum illumination," *Science*, vol. 321, no. 5895, pp. 1463–1465, Jan. 2008.

[2] Y. Yang, B. Yadin, and Z.-P. Xu, "Quantum-enhanced metrology with network states," *Phys. Rev. Lett.*, vol. 132, no. 21, p. 210801, May 2024.

[3] T. J. Proctor, P. A. Knott, and J. A. Dunningham, "Multiparameter estimation in networked quantum sensors," *Phys. Rev. Lett.*, vol. 120, no. 8, p. 080501, Feb. 2018.

[4] G. Cariolaro, *Quantum Communications*. Switzerland: Springer International Publishing, 2015.

[5] A. Giani, M. Z. Win, and A. Conti, "Quantum sensing and communication via non-Gaussian states," *IEEE J. Sel. Areas Inf. Theory*, pp. 1–15, 2024, early access.

[6] W. Pfaff *et al.*, "Unconditional quantum teleportation between distant solid-state quantum bits," *Science*, vol. 345, no. 6196, pp. 532–535, Aug. 2014.

[7] S. Guerrini, M. Z. Win, M. Chiani, and A. Conti, "Quantum discrimination of noisy photon-added coherent states," *IEEE J. Sel. Areas Inf. Theory*, vol. 1, no. 2, pp. 469–479, Aug. 2020, special issue on *Quantum Information Science*.

[8] T. Zanon-Willette, F. Impens, E. Arimondo, D. Wilkowski, A. V. Taichenachev, and V. I. Yudin, "Engineering quantum control with optical transitions induced by twisted light fields," *Phys. Rev. A*, vol. 108, no. 4, p. 043513, Oct. 2023.

[9] M. Clouâtré, S. Marano, P. L. Falb, and M. Z. Win, "Admissible optimal control for parameter estimation in quantum systems," *IEEE Control Syst. Lett.*, vol. 8, pp. 2283–2288, 2024.

[10] J. Liu and H. Yuan, “Quantum parameter estimation with optimal control,” *Phys. Rev. A*, vol. 96, no. 1, p. 012117, Jul. 2017.
[11] N. Maring *et al.*, “A versatile single-photon-based quantum computing platform,” *Nat. Photonics*, vol. 18, no. 6, pp. 603–609, 2024.
[12] S. Lloyd and S. L. Braunstein, “Quantum computation over continuous variables,” *Phys. Rev. Lett.*, vol. 82, no. 8, pp. 1784–1787, Feb. 1999.
[13] M. Gu, C. Weedbrook, N. C. Menicucci, T. C. Ralph, and P. van Loock, “Quantum computing with continuous-variable clusters,” *Phys. Rev. A*, vol. 79, no. 6, p. 062318, Jun. 2009.
[14] J. Illiano, M. Caleffi, A. Manzalini, and A. S. Cacciapuoti, “Quantum Internet protocol stack: A comprehensive survey,” *Computer Networks*, vol. 213, p. 109092, Aug. 2022.
[15] A. S. Cacciapuoti, M. Caleffi, R. Van Meter, and L. Hanzo, “When entanglement meets classical communications: Quantum teleportation for the Quantum Internet,” *IEEE Trans. Commun.*, vol. 68, no. 6, pp. 3808–3833, Jun. 2020.
[16] W. Dai, T. Peng, and M. Z. Win, “Optimal remote entanglement distribution,” *IEEE J. Sel. Areas Commun.*, vol. 38, no. 3, pp. 540–556, Mar. 2020, special issue on *Advances in Quantum Communications, Computing, Cryptography and Sensing*.
[17] M. Pant *et al.*, “Routing entanglement in the quantum internet,” *npj Quantum Inf.*, vol. 5, no. 1, pp. 1–9, Mar. 2019.
[18] L. Hanzo *et al.*, “Quantum information processing, sensing, and communications: Their myths, realities, and futures,” *Proc. IEEE*, pp. 1–51, 2025.
[19] S. Lloyd, J. H. Shapiro, F. N. C. Wong, P. Kumar, S. M. Shahriar, and H. P. Yuen, “Infrastructure for the quantum Internet,” in *ACM SIGCOMM Computer Commun. Review*, vol. 34, no. 5, New York, NY, USA, Oct. 2004, pp. 9–20.
[20] C. Weedbrook *et al.*, “Gaussian quantum information,” *Rev. Mod. Phys.*, vol. 84, pp. 621–669, May 2012.
[21] R. J. Glauber, “The quantum theory of optical coherence,” *Phys. Rev.*, vol. 130, pp. 2529–2539, Jun. 1963.
[22] B. R. Mollow and R. J. Glauber, “Quantum theory of parametric amplification. I,” *Phys. Rev.*, vol. 160, pp. 1076–1096, Aug. 1967.
[23] M. Reichert, R. Di Candia, M. Z. Win, and M. Sanz, “Quantum-enhanced doppler lidar,” *npj Quantum Inf.*, vol. 8, no. 1, p. 147, Dec. 2022.
[24] S.-H. Tan *et al.*, “Quantum illumination with Gaussian states,” *Phys. Rev. Lett.*, vol. 101, p. 253601, Dec. 2008.
[25] H. Aghaee Rad *et al.*, “Scaling and networking a modular photonic quantum computer,” *Nature*, Jan. 2025.
[26] C. L. Degen, F. Reinhard, and P. Cappellaro, “Quantum sensing,” *Rev. Mod. Phys.*, vol. 89, no. 3, p. 035002, Jul. 2017.
[27] K. C. Tan and H. Jeong, “Nonclassical light and metrological power: An introductory review,” *AVS Quantum Sci.*, vol. 1, no. 1, p. 014701, Nov. 2019.
[28] M. F. Sacchi, “Optimal discrimination of quantum operations,” *Phys. Rev. A*, vol. 71, no. 6, p. 062340, Jun. 2005.
[29] S. Guerrini, M. Z. Win, and A. Conti, “Photon-varied quantum states: Unified characterization,” *Phys. Rev. A*, vol. 108, no. 2, p. 022425, Aug. 2023.
[30] J. Fadrný, M. Neset, M. Bielak, M. Ježek, J. Bílek, and J. Fiurášek, “Experimental preparation of multiphoton-added coherent states of light,” *npj Quantum Inf.*, vol. 10, no. 1, p. 89, Sep. 2024.
[31] K. Wakui, H. Takahashi, A. Furusawa, and M. Sasaki, “Photon subtracted squeezed states generated with periodically poled KTiOPO4,” *Opt. Express*, vol. 15, no. 6, pp. 3568–3574, Mar. 2007.
[32] A. Zavatta, V. Parigi, and M. Bellini, “Experimental nonclassicality of single-photon-added thermal light states,” *Phys. Rev. A*, vol. 75, no. 5, p. 052106, May 2007.
[33] A. Zavatta, S. Viciani, and M. Bellini, “Quantum-to-classical transition with single-photon-added coherent states of light,” *Science*, vol. 306, no. 5696, pp. 660–662, Oct. 2004.
[34] A. Giani, M. Z. Win, and A. Conti, “Quantum discrimination of noisy photon-subtracted squeezed states,” in *Proc. IEEE Global Telecomm. Conf.*, Dec. 2022, pp. 5826–5831.
[35] Y. Ouyang, S. Wang, and L. Zhang, “Quantum optical interferometry via the photon-added two-mode squeezed vacuum states,” *J. Opt. Soc. Am. B*, vol. 33, no. 7, pp. 1373–1381, Jul. 2016.
[36] P. Hayden, D. W. Leung, and A. Winter, “Aspects of generic entanglement,” *Commun. Math. Phys.*, vol. 265, no. 1, pp. 95–117, 2006.
[37] P. V. P. Pinheiro and R. V. Ramos, “Quantum communication with photon-added coherent states,” *Quantum Inf. Process.*, vol. 12, no. 1, pp. 537–547, 2013.
[38] S. Guerrini, M. Chiani, and A. Conti, “Secure key throughput of intermittent trusted-relay QKD protocols,” in *Proc. IEEE Workshop on Quantum Commun. and Inf. Technol. (QCIT), Global Telecomm. Conf.*, Abu Dhabi, UAE, Dec. 2018, pp. 1–5.
[39] E. Villasenor, M. He, Z. Wang, R. Malaney, and M. Z. Win, “Enhanced uplink quantum communication with satellites via downlink channels,” *IEEE Trans. Quantum Eng.*, vol. 2, pp. 1–18, Jun. 2021.
[40] A. Giani, M. Z. Win, and A. Conti, “Quantum quadrature amplitude modulation with photon-added Gaussian states,” in *Proc. IEEE Global Telecomm. Conf.*, Kuala Lumpur, Malaysia, Dec. 2023.
[41] M. Endo *et al.*, “Non-Gaussian quantum state generation by multi-photon subtraction at the telecommunication wavelength,” *Opt. Express*, vol. 31, no. 8, pp. 12 865–12 879, Apr. 2023.
[42] Y. I. Bogdanov *et al.*, “Multiphoton subtracted thermal states: Description, preparation, and reconstruction,” *Phys. Rev. A*, vol. 96, no. 6, p. 063803, Dec. 2017.
[43] H. Groenewold, “On the principles of elementary quantum mechanics,” *Physica*, vol. 12, no. 7, pp. 405–460, 1946.